PCCP

Accepted Manuscript

ROYAL SOCIETY OF CHEMISTRY

www.rsc.org/pccp

Self-oriented β-Crystalline Phase in Poly (vinylidene fluoride) Ferroelectric and Piezo-sensitive Ultra-thin Langmuir-Schaefer Film

Subrata Maji,[a] *Piyush Kanti Sarkar,*[a] *Leena Aggarwal,*[b] *Sujoy Kumar Ghosh,*[c] *Dipankar Mandal,**[c] *Goutam Sheet,**[b] *and Somobrata Acharya**[a]

[a]Centre for Advanced Materials (CAM), Indian Association for the Cultivation of Science, Jadavpur, Kolkata 700032, India. Fax: +91-33-2473-2805; Tel: +91-33-24734971 (Ext. 1104); E-mail: camsa2@iacs.res.in

[b]Department of Physical Sciences, Indian Institute of Science Education and Research Mohali, Punjab, India, PIN: 140306; E-mail: goutam@iisermohali.ac.in

[c]Organic Nano-Piezoelectric Device Laboratory (ONPDL), Dept. of Physics, Jadavpur University, Kolkata 700032, E-mail: dipankar@phys.jdvu.ac.in

KEYWORDS: Poly (vinylidene fluoride); Langmuir-Schaefer Technique; Self-oriented *β*-Phase, Ferroelectric switching; Piezoelectric effect.

Abstract:

We report on the direct observation of ferroelectric switching and piezoelectric behaviour in ultrathin polyvinylidene fluoride (PVDF) films prepared by horizontal Langmuir-Schaefer (LS) technique. We have prepared pure β-phase by just increasing the number of LS layers without using additional non-ferroelectric assisting agent. Edge-on oriented CH_2/CF_2 units of PVDF at the air-water interface by means of hydrogen bonding network enable self-orientation of ferroelectric dipoles. Such restricted conformation of PVDF at the air-water interface results in the increase in net dipole moment with the number of LS layers. The ferroelectric switching and piezoelectric sensitivity are demonstrated by hysteretic polarization switching loops and butterfly-loops respectively. Successful circular domain writing on ultrathin LS film down to 5 monolayers of PVDF is demonstrated. Achievement of pure β-phase of PVDF at room temperature without using assisting agent may be found promising for non-volatile memory and piezoelectric based ultra thin smart sensor devices.

Introduction:

Ferroelectric polymers are in the centre of interest for a new generation of devices due to their unique properties. The polarization in ferroelectric polymers can be switched by an electric field, which is suitable for memory applications. In the recent past, interesting studies have been carried out on ferroelectric poly(vinylidene fluoride-co-trifuoroethylene), P(VDF-TrFE), a copolymer of polyvinylidene fluoride (PVDF) owing to thermodynamically stable ferroelectric β-phase (all *trans*, *i.e.*, *TTTT* conformation) which is suitable for non-volatile memories (*i.e.*, flash memory, FE-RAM, read only memory, etc.), piezo- and pyro-electric based sensors and

actuators (*i.e*., nanogenerators, anti-theft alarm, electronic skins, wireless biomedical sensors, microbalance, Braille display, robotic component, resonators, IR-sensors, etc.)[1,2] However, fatal thermal stability,[3] chemical reactivity, poor stacking integrity, limited ferroelectric dipole density and more importantly high cost of P(VDF-TrFE) are detrimental for large scale device fabrication.[4,5] Although, the presence of copolymerization units of TrFE is beneficial for high crystallinity,[6] often TrFE units causes current leaking paths due to crystal defects.[7] On the other hand, PVDF homopolymers exhibit superior properties like higher dipole density and thermal stability than P(VDF-TrFE), except the existence of room temperature stable β-phase rather exhibiting nonpolar and paraelectric α-phase (*TGTG′* conformation).[8] Therefore, tremendous effort has been paid to generate *β*-phase in PVDF, which includes traditional stretching method,[9] extreme thermal and pressure annealing,[10] application of electric field,[11] external additives,[12] and modified spin coating techniques.[13] However, in the most of the cases the full conversion of *β*-phase was not feasible and the semi-polar γ-phase (*TTTGTTTG′* conformation) co-exists which limits the ferroelectric memory functions. Recently it has been reported that δ-phase (polar version of α-phase) can exhibit superior memory functionality that is comparable with *β*-PVDF and P(VDF-TrFE) films.[4] It has been also found that the orientation of the ferroelectric dipoles (CH_2/CF_2-dipoles), *viz*., the edge-on orientation of the macromolecular PVDF chains is one of the important factors for reducing the operating voltage of the devices. However, electrical breakdown in the ultra thin films has been one of the major limiting factors.[4] Although the free-standing ferroelectric PVDF films are commercially available; however, fabrication of smooth ferroelectric *β*-PVDF thin film remains challenging. Commercially available ferroelectric films of several micrometers thickness require higher polarization switching field, which is expected to decrease for ultrathin PVDF films. The thinner films of ferroelectric polymers usually show

limited stack integrity in long range leading to degraded performance of the devices with the requirement of higher fields for polarization switching.

In this regard, the Langmuir-Blodgett (LB) technique is an advantageous method for sophisticated processability of 2D mono-molecular films since the packing, orientation and long-range ordering of the constituent monolayer can be precisely tailored with perfect control and reliable thickness.[14-19] Molecular level thin film can be formed at air-water interface for regular amphiphiles as well as nonamphiphilic molecules.[20,21] Though PVDF is not a classic amphiphilic in nature, however, it is possible to obtain a stable Langmuir monolayer by hydrogen bonding interaction between the water subphase and PVDF polymer to lock the all-trans conformation at air-water interface that may lead to high degree of self-oriented dipoles. Recently extrinsic switching characteristics of PVDF homopolymer films deposited by LB method was reported by Mitsuishi and co-workers.[6] Here additional amphiphilic poly (N-dodecylacrylamide) polymer along with PVDF polymer was required to lift up the PVDF film from the air-water interface. However, the use of non ferroelectric assisting agent may reduce overall ferroelectric performance and the surface quality of the film. Another recent report by Sun and co-workers[22] describes the transition of polarization switching in the ultrathin PVDF homopolymer films made by horizontal LS method. However, annealing at 145°C for 3 hours was employed to improve the β-phase crystallinity of the deposited films. Notably, the melting temperature of the PVDF is closer to 145°C, therefore it may induce permanent phase change from β to γ or α phases. Hence, the requirement is to develop stable β-phase with the higher yield within the ultrathin film of PVDF without annealing or without using external polymer.

Here we show that self-orientation of PVDF in full β-phase can be obtainable at the air-water interface without using any external agent, heating or polling which can be transformed

onto solid support using LS technique. The self-ordering of PVDF monolayer at the air-water interface was probed by measuring the surface potential using Kelvin probe. Fourier-transform infrared spectroscopy (FTIR) measurements reveal that fully converted β-phase can be achieved just by increasing the number of monolayers of PVDF by sequential transfer from air-water interface using LS deposition cycle. We show ferroelectric domain switching of nanometer thin PVDF film down to 5 monolayers by using piezoresponse force microscopy (PFM). The butterfly-loops suggest piezoelectric behaviour of the PVDF LS films. The room temperature ferroelectric properties are correlated with the molecular self-orientation of PVDF at the air-water interface resulting in an effective increase of molecular dipole moments.

Experimental Section:

Materials: PVDF (M_n = 7.1 × 10^4, M_w = 1.8 × 10^5) and dimethylformamide (DMF) was purchased from Sigma Aldrich and used without any purification.

Langmuir Trough Experiments: A Langmuir trough from Nima Technologies was used for all experiments at the air-water interface. PVDF was dissolved in DMF at room temperature to make a solution of concentration of 0.5 wt% (w/v). Ultra pure milli-Q water (18 MΩ-cm) from Merk Millipore system was used as subphase for LB experiment. 300 µl solution of PVDF in DMF was spread at air-water interface and 30 minutes for solvent evaporation as well as monolayer equilibration was allowed. The barrier was compressed at a speed of 10 cm^2/minute to record the surface pressure (π) versus area per monomer unit (A) isotherm at room temperature (22°C). Surface potentials at the air-water interface were measured using Trek Electrometer 320. The same volume of PVDF solution was spread for surface potential measurements at the air-water interface. Monolayer and multilayer PVDF films were lifted from

air-water interface by Langmuir-Schaefer (LS) method on top of silicon wafer for FTIR measurement as well as on freshly cleaved mica and ITO coated glass substrate for piezo force microscopy (PFM) and atomic force microscopy (AFM) measurements.

FTIR Measurement: FTIR spectra of PVDF films on clean silicon wafer lifted by LS method from air-water interface were recorded at room temperature with a Series II Magna-IR model 750 spectrometer from Nicolet Instrument Corporation (Madison, WI). In all cases, spectra were taken in absorption mode and the data were averaged over 100 scans. The resolution of the instrument was 4 cm^{-1}.

Piezoresponse Force Microscopy (PFM): The piezo-response force microscopy measurements were performed in an Asylum Research AFM (MFP-3D) with an additional high-voltage amplifier. For these measurements, a conducting AFM cantilever (spring constant = 2 N/m, free air resonance frequency = 70 kHz) with a Pt-Ir coated tip mounted on it was brought in contact with the LS films. A small ac excitation (V_{ac} = 3 V) riding on a dc bias voltage (V_{dc}) was applied between the tip and the amplifier ground. The response of the sample to the applied modulating field was measured through the reflection of a laser beam from the cantilever that was recorded by a position sensitive photo-diode, as in a regular atomic force microscope.

Result and Discussion:

Pressure-Area Isotherm and FTIR: PVDF and its copolymers are not amphiphilic rather hydrophobic in nature; however, they can form stable monolayer at air-water interface. Figure 1a shows the surface pressure (π) versus area per monomer unit (A) isotherm of pure PVDF at the air-water interface taken at room temperature (22^{o}C). The π-A isotherm clearly shows a gaseous

phase at initial stage of compression which is followed by the liquid-expanded and liquid-condensed phases. The extrapolation of the liquid-condensed region to the zero surface pressure reveals a limiting molecular area of 0.012 nm^2/monomer unit which is close to the literature value.[23] Surface potential measurement of the monolayer is a useful technique for the study of

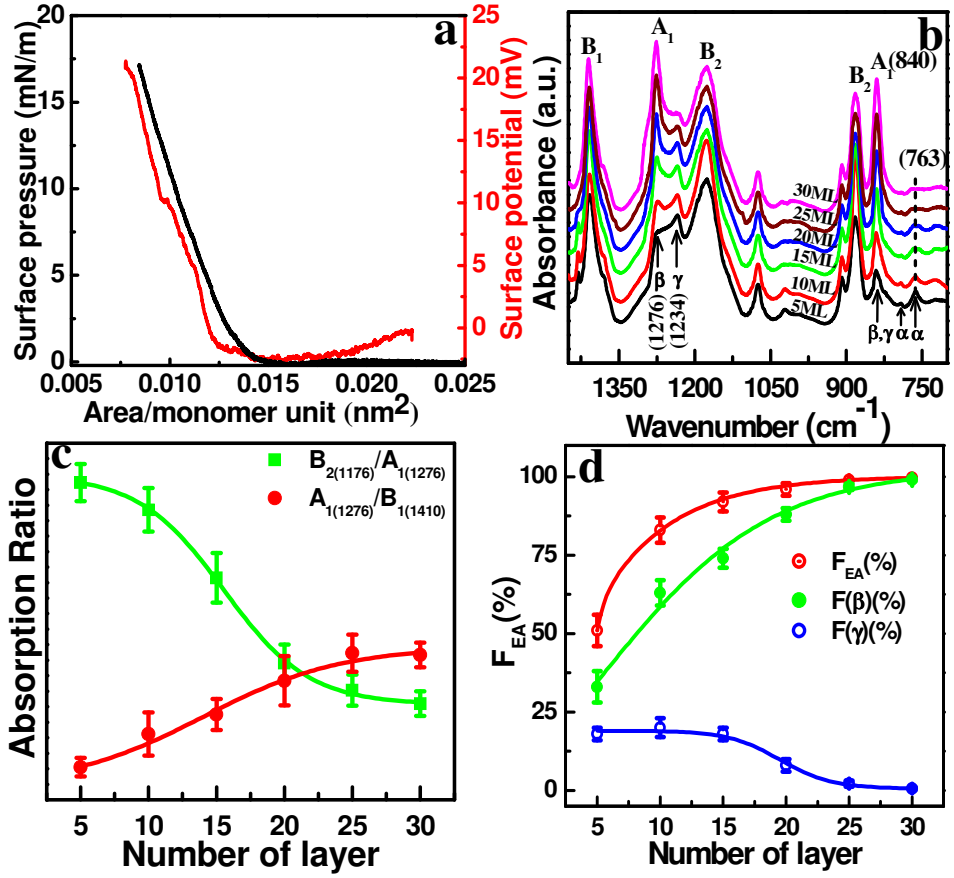

Figure 1. (a) Pressure-Area isotherm (black curve) as well as surface potential-Area isotherm (red curve) of pure PVDF polymer on milli-Q water subphase at room temperature (22°C). (b) FTIR spectrum of pure PVDF film with increasing monolayer number: 5 monolayers (black curve), 10 monolayers (red curve), 15 monolayers (green curve), 20 monolayers (blue curve), 25 monolayers (wine curve) and 30 monolayers (magenta curve). (c) The absorption ratio of $B_{2(1176)}/A_{1(1276)}$ and $A_{1(1276)}/B_{1(1410)}$ deduce from FTIR spectra. (d) The percentage of F_{EA}, $F(\beta)$ and $F(\gamma)$ of PVDF films as a function of number of monolayer calculated from FTIR spectra.

reorganization processes of molecular dipoles within the Langmuir monolayer.[24] Figure 1a shows the change in the surface potential with the area per monomer of the PVDF Langmuir monolayer. The effective molecular dipole moment at the air-water interface is defined as the product of the change in the surface potential (ΔV) and the average area per monomer (A).[25] Using this simplified form, the influence of the orientational change within the monolayer of PVDF between the electrodes of the Kelvin probe is estimated. At the beginning of compression, almost no change in the surface potential with the change in the area is observed. A rapid compression-induced increase of the effective molecular dipole moment is observed at higher surface pressure which indicates that the PVDF molecules are oriented in such a way that the effective dipole moment is perpendicular with respect to the air-water interface. A possible orientation of PVDF molecules at the air-water interface is presented in figure 2a based on the surface potential measurements. We postulate that the CH_2 units of the individual PVDF chain are attached with the water molecule through H-bonding interaction which pushes CF_2 units upward towards the air. This self-orientation at the air-water interface leads to complete all-trans conformation i.e. the β-phase at higher surface pressures. Within the locked conformation at the liquid condensed phase, the direction of the CH_2-CF_2 dipoles are perpendicular with respect to the air-water interface and results in oriented dipole moment within a compact monolayer as evidenced from the surface potential measurements. This gives rise to the sudden increase in the surface potential when the PVDF moieties come into closer proximity with the aid of the surface pressure. Notably, the conformation of PVDF molecules at the air-water interface is different from a previous report which predicts CF_2 parts of the PVDF chain form H-bonding with the water molecules.[26] However, it is accepted that hydrogen bond formation of water molecules with CF_2 units of PVDF molecules is unlikely principle even considering more electronegativity

of CF_2 in comparison to CH_2 units. Hence, we propose the LS monolayer transfer onto the solid substrate as shown in figure 2b. The PVDF chains remain in edge-on conformation during the monolayer LS film deposition on top of silicon wafer where the direction of the CH_2-CF_2 dipoles remains perpendicular with respect to the silicon wafer. During the second cycle of LS film deposition, the exposed CH_2 units of first monolayer interact with the CF_2 units through electrostatic interaction resulting in the next monolayer transfer (figure 2c). This electrostatic interaction is feasible considering the relatively positive charge density of CH_2 moieties than CF_2 units of PVDF. This transfer process onto solid substrate orients the direction of the CH_2-CF_2 dipoles in a direction perpendicular to the silicon wafer. Hence, the successive LS monolayer transfer increase the net dipole moment resulting in increase of electroactive phases (F_{EA}) with increasing layer numbers as reflected in the FTIR (figure 1b).

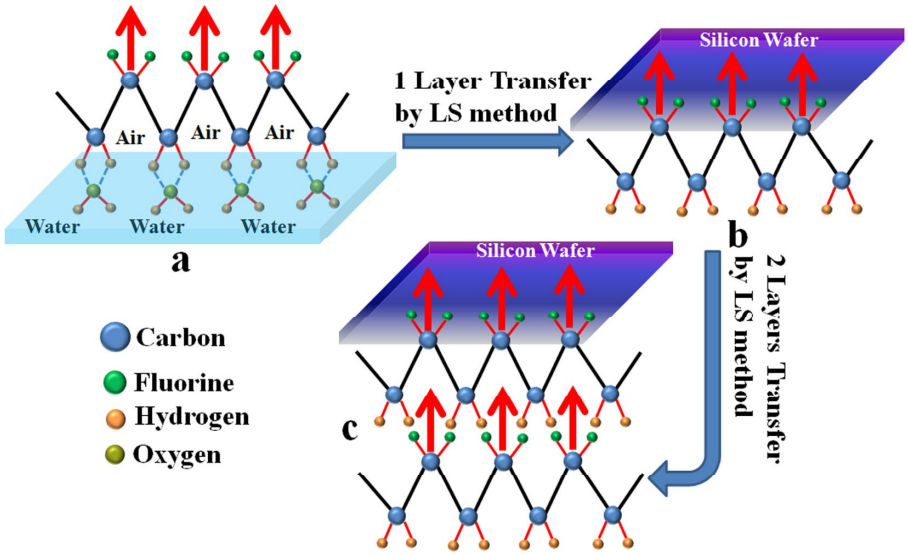

Figure 2. (a) Complete edge-on type conformation of the PVDF at air-water interface where CH_2-CF_2 dipoles (shown by red arrows) remain perpendicular with respect to air-water interface. (b) One LS monolayer transferred on top of silicon wafer with CH_2-CF_2 dipoles direction shown by red arrows. (c) Two monolayers transferred on top of silicon wafer with CH_2-CF_2 dipoles direction shown by red arrows showing an increase in the net dipole moment.

Notably, the surface potential curve retraces the π-A isotherm curve indicating the same orientation conformation of PVDF molecules at the air-water interface with respect to the applied surface pressure. The π-A isotherm and the surface potential isotherm clearly reveal that the most compact monolayer can be obtainable within the surface pressure ranging from 15 to 20 mN/m at the air-water interface. Hence, mono- and multilayer of PVDF films were lifted at a surface pressure 16 mN/m by LS method on top of solid support. Figure 1b shows FTIR spectra of PVDF film on silicon wafer with different number of layers. The presence of non-polar α-phase is assigned from the presence of strong peaks at 763 and 792 cm^{-1} respectively,[27] whereas peaks at 1276 cm^{-1} (A_1 symmetry) and 1234 cm^{-1} indicate that 5 monolayers LS film bears of some amount of *β* and γ-phases. [28,29] However, a large promotion of *β*-phase with continues decrease of γ-phase with increasing number of monolayer can be directly visualized from FTIR spectra (Figure 1b). Finally, a complete conversion into *β*-phase with a negligible amount of γ-phase and without any trace amount of α-phase is evidenced in 30 monolayers PVDF film. Hence, a paraelectric phase of PVDF can be completely converted into oriented ferroelectric phase just by increasing the number of monolayer of LS films without using external temperature, pressure, electrical poling or any assisting agent.

The well-known relationship between the vibrational transition moment (μ) and the unit cell axes (a, b, c) of the *β* crystal and each vibrational symmetry species (A_1, B_1, and B_2 as shown in figure 1b) is related by μ∥b at A_1, μ∥c at B_1, and μ∥a at B_2.[29] As per the structure of β-crystal unit cell, the A_1 band at 1276 cm^{-1} ($\nu_s CF_2$ coupled with $\nu_s CC$ and $\delta_s CCC$) is highly sensitive to the *β*-crystalline modification, whereas the B_2 band at 883 cm^{-1} ($\nu_s CF_2$ coupled with $\nu_s CC$ and $\delta_s CCC$)

and another B_2 band at 1176 cm^{-1} coupled with $\nu_s CF_2$ and tCH_2 are insensitive in β-crystalline orientation. Initially, B_1 band at 1410 cm^{-1} (coupled with $\nu_{as}CC$ and ωCH_2) intensity is found to be higher than $A_{1(1276)}$ in 5 monolayers LS PVDF film indicating the predominance of face-on type crystalline lamella. In contrast, $A_{1(1276)}/B_{1(1410)}$ ratio is further increased with increasing the number up to 30 monolayers (figure 1c). The complete edge-on type crystalline lamella formation in 30 monolayers LS film is evidenced from the higher intensity of $A_{1(1276)}$ in comparison to $B_{1(1410)}$. The increase in β phase is attributed to the strong hydrogen bonding

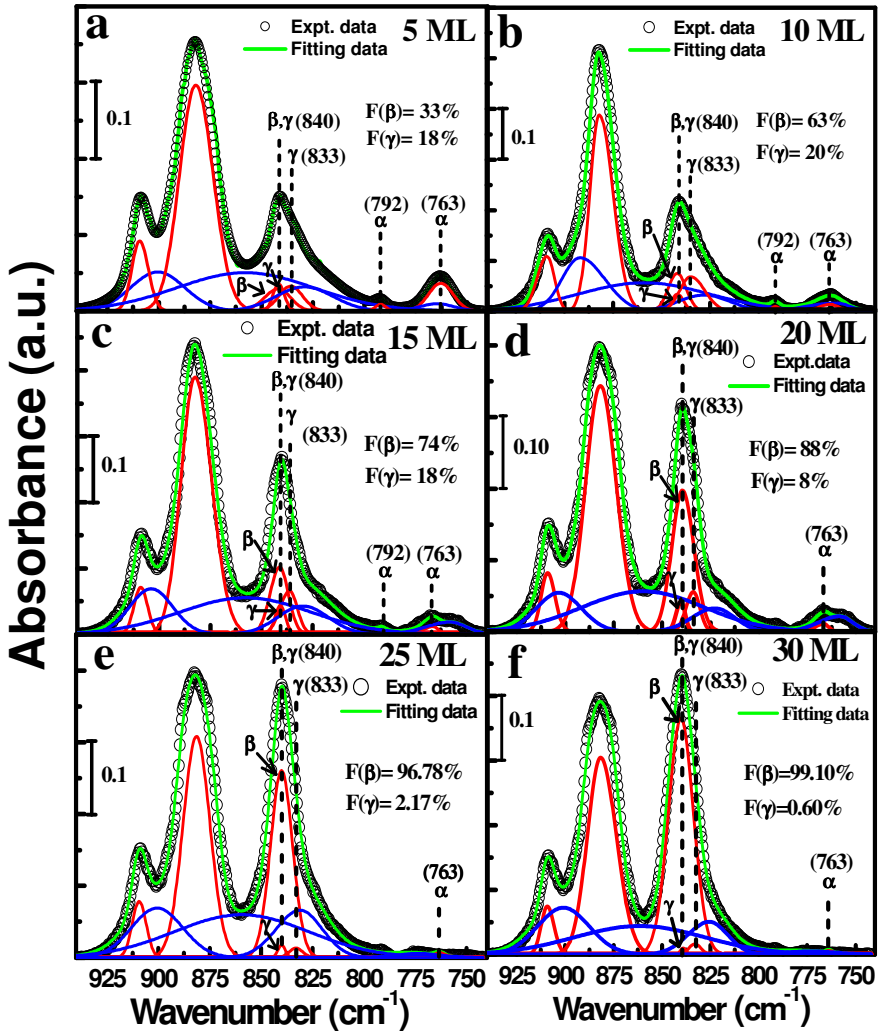

Figure 3. The deconvolution of the FTIR spectra (940-740 cm^{-1}) of PVDF LS films with different monolayer as mentioned in the figure. The calculated percentage of individual *F(β)* and *F(γ)* is mentioned in the inset. "ML" stands for monolayer.

interaction promoting the edge-on type crystalline lamella orientation. In addition, the reduced intensity ratio of $B_{2(1176)}/A_{1(1276)}$ and finally the higher intensity of $A_{1(1276)}$ in comparison to $B_{2(1176)}$ in 30 monolayers film is another direct consequence of full edge-on type crystalline lamella formation (figure 1c). The consequence of figure 1d is represented in the following section. For quantification of relative proportion of electroactive β and γ-phases, we have deconvoluted the FTIR spectra (900-750 cm^{-1} regions) obtained for different number of LS monolayers (Figure 3a-3f).[12] Note that, A_1 at 840 cm^{-1} (coupled with $\nu_s CF_2$ and νCC) is not comparable with $B_{1(1410)}$ band as $A_{1(840)}$ convey the dual characteristic of *β* and γ-crystalline phases. Only $A_{1(1276)}$, $B_{1(1410)}$ and $B_{2(1176)}$ can be compared because of their comparable absorption coefficients. However, the absorption intensity at 840 cm^{-1} band can be assigned to quantify the relative proportion of electroactive phases (F_{EA}) attributing to both *β* and γ-phases using the following equation:

$$F_{EA} = \frac{I_{EA}}{(\frac{K_{840}}{K_{763}})I_{763} + I_{EA}} \times 100 \quad \text{..... (1)}$$

Where, $\boldsymbol{I_{763}}$ and $\boldsymbol{I_{EA}}$ are the absorbance intensity at 763 and 840 cm^{-1} respectively; $\boldsymbol{K_{763}}$ and $\boldsymbol{K_{840}}$ are the absorption coefficients at the respective wavenumbers.[30] Figure 1d shows that the fraction of electroactive phase (F_{EA}) increases significantly from ~50% for 5 monolayers LS film to ~99% for 30 monolayers LS film.

The individual β and γ-phases for different layer numbers of LS PVDF films is also performed by curve deconvolution of 840 cm^{-1} band (Figure 3), where the broadening contribution due to γ-phase and sharp well resolved peak for β-phase have been considered. The following equations are adopted to quantify the relative proportion of electroactive β and γ-phases individually.[12]

$$F(\beta) = F_{EA} \times \left(\frac{A_\beta}{A_\beta + A_\gamma}\right) \times 100 \quad \text{..... (2a)}$$

$$F(\gamma) = F_{EA} \times \left(\frac{A_\gamma}{A_\beta + A_\gamma}\right) \times 100 \quad \text{..... (2b)}$$

Where, A_β and A_γ are the integrated area under the β and γ marked deconvoluted curves in Figure 3 for different layer numbers centred at 840 cm^{-1} band. The individual quantification of $F(\beta)$ and $F(\gamma)$ are denoted in the inset of Figure 3 from 5 monolayers to 30 monolayers respectively. The plot of $F(\beta)$ and $F(\gamma)$ with respect to the number of layers (Figure 1d) clearly reveals an increase in $F(\beta)$ and a decrease in $F(\gamma)$ with increase in the number of LS layers. Figure 3 shows that the Gaussian peak (marked by arrow) corresponding to β-phase (centred at 840 cm^{-1}) is more pronounced with higher layer numbers whereas, the Gaussian peak (marked by another arrow) corresponding to γ-phase (centred at 840 cm^{-1}) is gradually weakened with higher layer numbers and finally almost vanishes for 30 monolayers PVDF LS film. For lower number of LS layers, the additional contribution from γ-phase along with the β-phase to the relative proportion of electroactive phases (F_{EA}) is clearly evidenced. However, for 30 monolayers LS film, there is negligible contribution from γ-phase to F_{EA}, rather $F(\beta)$ becomes saturated to the maximum (Figure 1d) indicating full conversion of oriented β-phase from non-polar α-phase and anisotropic electroactive phases (*i.e.* β- and γ-phase). Thus, we have successfully achieved ~99%

of proportional β-phase for 30 monolayers starting from ~33% for 5 monolayers without using any assisting agent or without any heating.

The surface morphologies of the PVDF films lifted by LS method on top of freshly cleaved mica at surface pressure of 16 mN/m was obtained by contact mode AFM measurements. The AFM topography images of LS films with different number of layers along with the corresponding root-mean-square (RMS) roughness are presented in Figure 4. The topography analysis reveals that the compact film of PVDF over ~36 μm^2 can be easily

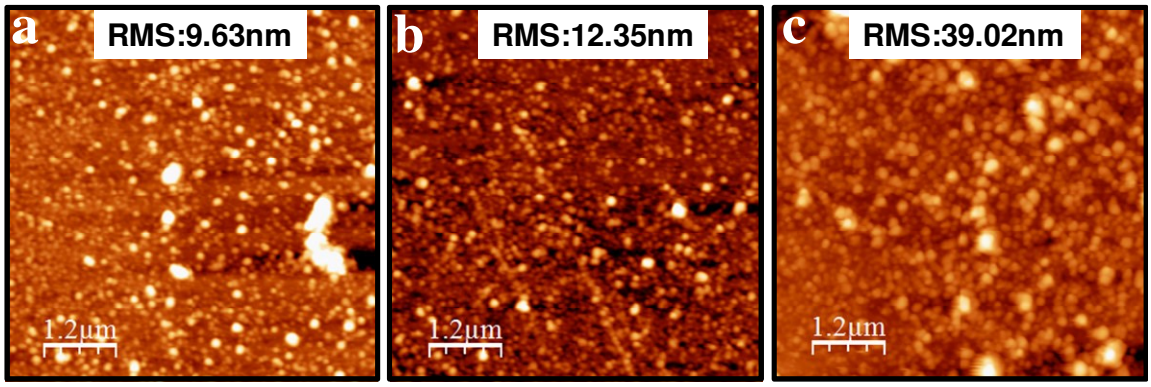

Figure 4. AFM topography images with corresponding root means square (RMS) roughness of PVDF with different monolayer on top of freshly cleaved mica lifted by LS method at surface pressure 16mN/m: (a) 5 monolayers (b) 10 monolayers and (c) 30 monolayers. RMS roughness was calculated for the full area of the images.

obtainable using the LS transfer process. Importantly, the compactness of the films is found to increase with increasing the number of layers indicating a regular transfer of the monolayer by LS process. Although, the RMS roughness of the LS films increases with increasing the layer number, however, the RMS roughness for our LS films is found to be ~50% less than that reported previously.[6,23]

In order to investigate the local ferroelectric and piezoelectric properties of the PVDF LS films, we have employed piezoresponse force microscopy (PFM). The LS films lifted on cleaved mica and ITO surfaces were loaded on a conducting sample holder that is directly connected to the ground of the high voltage amplifier used for the PFM measurements (see experimental section for details). The PFM phase responses reveal a clear hysteresis in phase versus dc bias (V_{dc}) diagram (Figure 5). The phase switches sharply at V_{dc} = 30V by ~180° with a coercive voltages of ±9V for 5 layers, ±5V for 10 layers (Figure 5a), ±16V for 20 layers and ±17V for 30

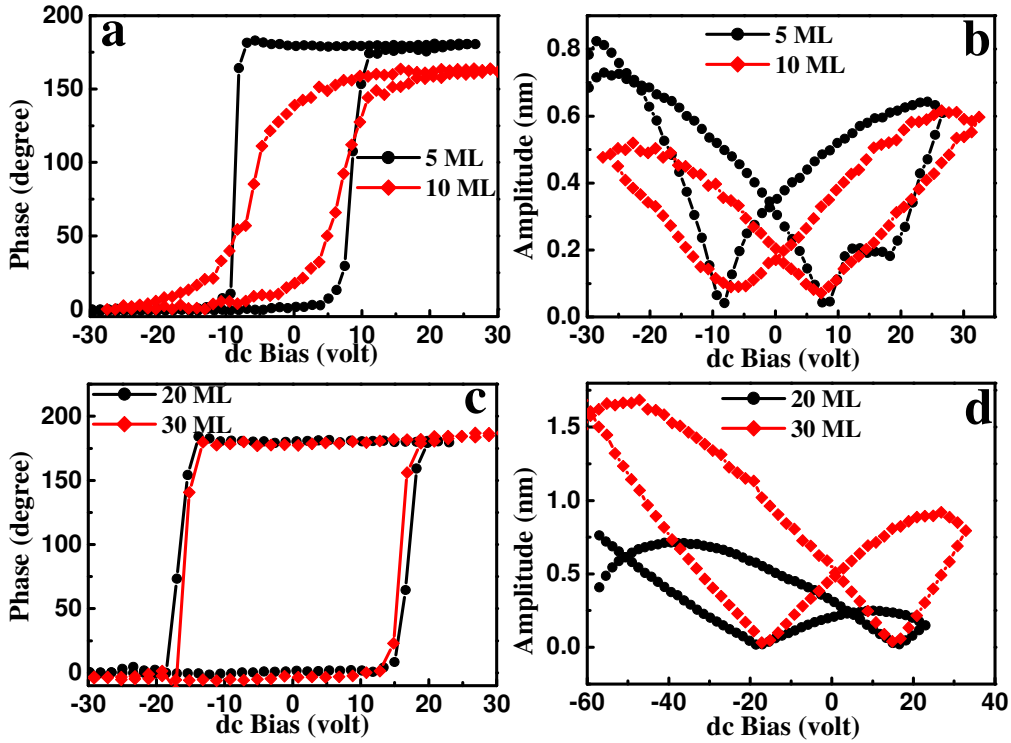

Figure 5. PFM phase-voltage and amplitude-voltage hysteresis loops of PVDF film with different number of monolayers: (a) Phase-voltage hysteresis loops for 5 monolayers (black curve) and 10 monolayers (red curve) on top of mica substrate. (b) Corresponding "Butterfly" loop for 5 monolayers (black curve) and 10 monolayers (red curve). (c) Phase-voltage hysteresis loops for 20 monolayers (black curve) and 30 monolayers (red curve) on top of ITO substrate. (d) Corresponding "Butterfly" loop for 20 monolayers (black curve) and 30 monolayers (red curve). In the inset, "ML" stands for monolayer.

layers (Figure 5c) of LS films respectively. The coercive voltages for 30 and 20 monolayers LS films are found to be almost same, while the coercive voltage for 5 monolayers LS film is greater than that of 10 monolayers LS film. Notably, the phase of the PFM response signal is directly related to the direction of the electric polarization of the microscopic region of the surface monitored under the tip. Thus, the switching of the phase of the response signal hysteretically by 180° in response to a sweeping DC voltage is attributed to the switching of the direction of polarization of the dipoles of PVDF along the direction of the electric field. This implies that the hysteretic 180° phase switching observed in the PFM response is an evidence of local ferroelectricity of the PVDF films. The amplitude (*A*) of the response signal in PFM is directly related to the local strain of PVDF film experienced by the cantilever. The amplitude (A) versus V_{dc} curves are also hysteretic and the shape of the loops strongly resemble the "butterfly loop" normally observed in piezoelectrics (Figure 5b and 5d).[31] The amplitude (A) versus V_{dc} loop was measured by applying a voltage of -30V to +30V for 5 monolayers and 10 monolayers (figure 5b) and -60V to +30V for 20 monolayers and 30 monolayers (figure 5d) to the tip with respect to the ground. At -30V (greater than the coercive voltage, figure 5b), all the dipoles underneath the tip are parallel to the applied field. With decrease in negative voltage (i.e. changing from -30V to 0V), the amplitude decreases due to contraction of the LS film. As the applied voltage changes from negative to positive crossing 0V, the field becomes antiparallel with the dipoles underneath the tip. Hence, an increase in the field causes the dipoles to contract resulting in a decrease in the amplitude. When the voltage reaches to the coercive value (+9V in figure 5b), the dipoles underneath the tip switched to opposite direction causing a 180° phase change. At this stage, the dipoles underneath the tip are parallel to the field direction. An

increase in the applied field causes increase of the amplitude due to dipole expansion, which reaches to the highest level at +30V. A decrease of the applied field at this stage causes the amplitude to decrease due to the dipole contraction which continues up to 0V. A reversal of field direction becomes antiparallel to the dipoles causing the dipoles to contract with further increase of the field. As the voltage reaches to negative coercive value (-9V for figure 5b), it changes the polarization of the dipoles to 180^{o} until the voltage reaches to the maximum (-30V) causing expansion of the LS film underneath of the tip. From the slope of the piezoelectric amplitude (A) versus V_{dc} curves, we have calculated the effective piezoelectric coefficient (d_{33}) values for different number of layers.[32,33] Effective d_{33} values appear to be ~ 47.7pm/V, ~ 20pm/V, ~ 22.5pm/V and ~ 50pm/V for 30 monolayers, 20 monolayers, 10 monolayers and 5 monolayers respectively. The observations of hysteretic phase switching and butterfly loops indicate that the PVDF LS films possess ferroelectric and piezoelectric properties. Notably, hysteretic effects in PFM phase and amplitude may also arise from electrostatic and electrochemical effects.[34] In order to minimize the role of the electrostatic effects, all the measurements were performed following SS-PFM (switching spectroscopy piezoresponse force microscopy) pioneered by Jesse et al.[35] In this method, V_{dc} is applied in sequence of pulses instead of sweeping V_{dc} continuously, while the phase and amplitude measurements are done in the "off-state" of the pulses. We have observed a significant difference in the "off-state" results in comparison to the "on-state" measurements, which indicates that the electrostatic effects have been minimized in the "off-state" measurements. Hence, we rule out the electrostatic effect on the hysteretic effects exhibited by PVDF films. The possibility of electrochemical reactions under the tip is ruled out by topographic imaging after the spectroscopic measurements, where we do not observe any topographic modification that is usually expected to result from tip-induced electrochemical

processes as shown in figure 6a and 6c. The common way to confirm ferroelectricity of PVDF and its copolymers is to measure hysteresis loop of polarization (P) verses electric field (E). However, measurement of P-E loop requires certain film thickness in bulk measurement conditions and measurements of nanometer thin films become exceedingly critical. In addition to the hysteretic switching effects, the observation of domains on the PVDF surface is unambiguous proof of ferroelectricity.

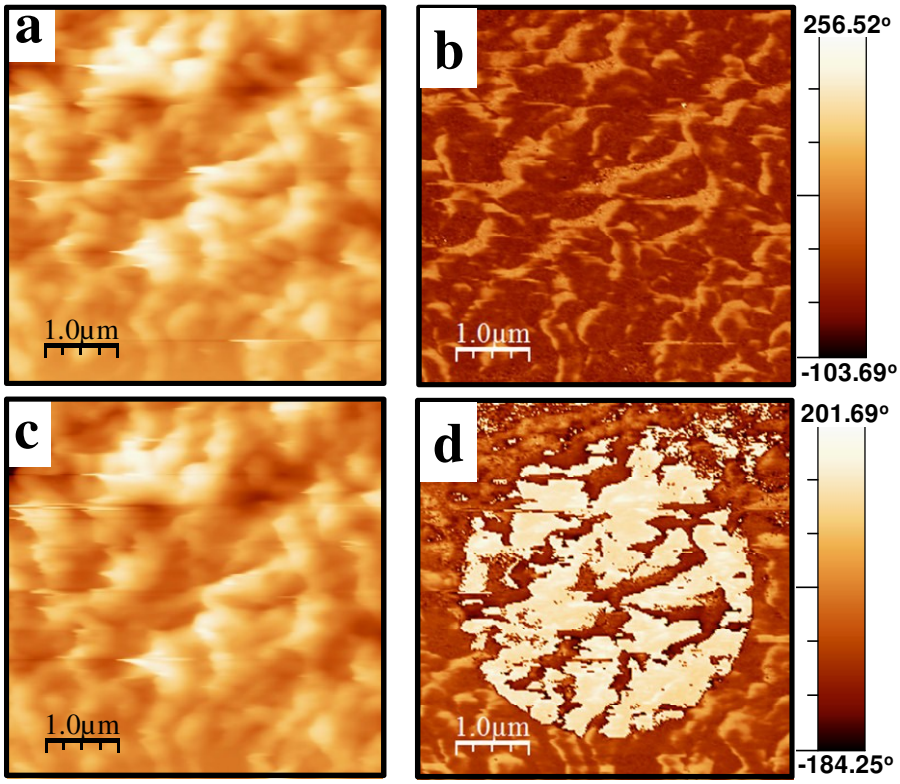

Figure 6. PFM images of PVDF 5 monolayers film lifted by LS method on top of freshly cleaved mica. (a) PFM topography image before writing the domain and (b) corresponding PFM phase image before writing the domain. (c) PFM topography image after writing the circular domain and (d) corresponding PFM phase image after writing the circular domain.

Hence, we employed piezoresponse force microscopy (PFM) to directly measure the piezoelectric hysteresis loops of individual continues domains of PVDF.[1] For PFM imaging, first

the contact-mode resonance of the cantilever was measured by bringing the tip in contact with LS film surface and then recording the amplitude response of the cantilever as function of the frequency of V_{ac}. After that, the tip was scanned on the surface of the film with a constant deflection recorded by a photodiode. The plot of the phase of the response signal as a function of the position of the tip on the LS film surface represents a map of the distribution of the directional orientation of the electric polarization on the film. A phase shift of 180° is expected if positive and negative polarization vectors are present in two different domains within the LS film. Therefore, the phase map is nothing but the map of the ferroelectric domains distributed on the film. Since the measurement is likely to be affected by the change in the contact-mode resonance frequency as the tip scans on the surface, all the imaging were done in the dual ac-resonance tracking (DART)-mode of PFM, where a dedicated feedback loop always kept the cantilever in resonance during the scans. It should be noted that in the PFM imaging method, we have recorded the vertical amplitude and phase response. The images thus results in the information about the components of electric polarization along the directions parallel and antiparallel to the axis of the tip. Figure 6 shows the topography (figure 6a and 6c) and phase (figure 6b and 6d) images for 5 monolayers LS film. Figure 6b is the phase image of the selected area before the polling showing almost same phase within the LS film throughout the entire image. Figure 6d represents the phase image of the same area after the polling which clearly shows a circular color contrast suggesting that the dc bias switched the phase of the local domain of PVDF LS film almost by 180°.[36] We observe that the polarization did not occur perfectly in a small portion within the circular domain. We attribute this effect due to the variation of the thickness of the sample on that area. Increase in the thickness means decrease in the effective electric field as the bias voltage of the tip with respect to the ground is constant to 30V. Since the

tip is in contact with the film and moving on the film surface, a fixed bias voltage implies change in the resultant electric field with the change in film thickness. An increase in the thickness of the portion of the film will cause decrease in the resultant electric field, which correspondingly affects the polling of the domains. Earlier it was reported that ferroelectric imaging cannot be done on neat PVDF film even with the presence of electro-active β-phase.[29] However, our results unambiguously suggest that successfully domain writing is possible in thin 5 monolayers PVDF LS film (figure 6a and 6c). Thus, upward or downward polarization state can be denoted as "1" or "0", corresponding with the well-established binary memory system can directly be utilized in ferroelectric data storage device.

Conclusions:

In summary, we have prepared nanometer thin PVDF films by using very simple Langmuir-Schaefer method. From surface potential (ΔV) vs area (A) isotherm we can conclude that the molecular dipolemoments are perpendicular to the air-water interface i.e. PVDF polymer chains are in almost β-phase configuration. From FTIR study we can conclude that we achieved ~99% of β-phase proportion for 30 monolayers PVDF film starting from ~33% for 5 monolayers PVDF film without using any assisting agent or without any heating. We have confirmed the ferroelectric switching and piezoelectric behaviour of the nanometer thin Polyvinylidene fluoride (PVDF) films prepared by horizontal Langmuir-Blodgett method by using Piezoresponse Force Microscopy (PFM) technique. This type of nanometer thin film can be useful for low cost non-volatile memory.

Acknowledgment:

The work is supported by DST, India. G.S. gratefully acknowledges Ramanujan Fellowship from DST, India. S. M. gratefully acknowledges CSIR, India for fellowship. P. K. S. and S. K. G. gratefully acknowledge DST-INSPIRE fellowship.

References:

1. Z. Xiao, Q. Dong, P. Sharma, Y. Yuan, B. Mao, W. Tian, A. Gruverman and J. Huang, *Adv. Energy Mater.*, 2013, **3**, 1581.

2. Y. Yuan, P. Sharma, Z. Xiao, S. Poddar, A. Gruverman, S. Ducharmebc and J. Huang, *Energy Environ. Sci.*, 2012, **5**, 8558.

3. Y. J. Park, I. Bae, S. J. Kang, J. Chang and C. Park, *IEEE Trans. Dielectr. Electr. Insul.*, 2010, **17**, 1135.

4. M. Li, H. J. Wondergem, M. J. Spijkman, K. Asadi, I. Katsouras, P. W. M. Blom and D. M. D. Leeuw, *Nat. Mater.*, 2013, **12**, 433.

5. K. Asadi, M. Li, P. W. M. Blom, M. Kemerink and D. M. Leeuw, *Mater. Today*, 2011, **14**, 592.

6. H. Zhu, S. Yamamoto, J. Matsui, T. Miyashitaa and M. Mitsuishi, *J. Mater. Chem. C*, 2014, **2**, 6727.

7. S. Fujisakia, H. Ishiwara and Y. Fujisaki, *Appl. Phys. Lett*., 2007, **90**, 162902.

8. X. He and K. Yaoa, *Appl. Phys. Lett*., 2006, **89**, 112909.

9. A. Salimi and A. A. Yousefi, *Polymer Testing*, 2003, **22**, 699.

10. S. J. Kang, Y. J. Park, J. Sung, P. S. Jo, C. Parka, K. J. Kim and B. O. Cho, *Appl. Phys. Lett*., 2008, **92**, 012921.

11. S. W. Choi, J. R. Kim, Y. R. Ahn, S. M. Jo and E. J. Cairns, *Chem. Mater*., 2007, **19**, 104.

12. S. K. Ghosh, M. M. Alam and D. Mandal, *RSC Adv*., 2014, **4**, 41886.

13. H. J. Jung, J. Chang, Y. J. Park, S. J. Kang, B. Lotz, J. Huh and C. Park, *Macromolecules*, 2009, **42**, 4148.

14. S. Acharya, B. Das, U. Thupakula, K. Ariga, D. D. Sarma, J. Israelachvili and Y. A Golan, *Nano Lett.*, 2013, **13**, 409.

15. A. Riul, D. S. dos Santos, K. Wohnrath, R. Di Tommazo, A. C. P. L. F. Carvalho, F. J. Fonseca, O. N. Oliveira, D. M. Taylor and L. H. C. Mattoso, *Langmuir*, 2002, **18**, 239.

16. N. Belman, S. Acharya, O. K. A. Vorobiev, J. Israelachvili, S. Efrima and Y. Golan, *Nano Lett.*, 2008, **8**, 3858.

17. S. Acharya, D. Bhattacharjee and G. B. Talapatra, *Chem. Phys. Lett.*, 2003, **372**, 97.

18. K. Ariga, Y. Yamauchi, T. Mori and J. P. Hill, *Adv. Mater.*, 2013, **25**, 6477.

19. K. Ariga, T. Mori, S. Ishihara, K. Kawakami and J. P. Hill, *Chem. Mater.*, 2014, **26**, 519.

20. S. Maji, S. Kundu, L. F. V. Pinto, M. H. Godinho, A. H. Khan and S. Acharya, *Langmuir*, 2013, **29**, 15231.

21. S. Maji, A. Das, P. K. Sarkar, A. Metya, S. Ghosh and S. Acharya, *RSC Adv*., 2014, **4**, 44650.

22. J. L. Wang, B. L. Liu, X. L. Zhao, B. B. Tian, Y. H. Zou, S. Sun, H. Shen, J. L. Sun, X. J. Meng and J. H. Chu, *Appl. Phys. Lett*., 2014, **104**, 182907.

23. H. Zhu, M. Mitsuishi and T. Miyashita, *Macromolecules*, 2012, **45**, 9076.

24. M. Ferreira, C. J. L. Constantino, C. A. Olivati, M. L. Vega, D. T. Balogh, R. F. Aroca, R. M. Faria and N. O. Jr. Osvaldo, *Langmuir*, 2003, **19**, 8835.

25. P. C. Tchoreloff, M. M. Boissonnade, A. W. Coleman and A. Baszkin, *Langmuir*, 1995, **11**, 191.

26. S. Chen, X. Li, K. Yao, F. E. H. Tay, A. Kumar and K. Zeng, *Polymer*, 2012, **53**, 1404.

27. Y. Bormashenko, R. Pogreb, O. Stanevsky and E. Bormashenko, *Polymer Testing*, 2004, **23**, 791.

28. S. Ramsundaram, S. Yoon, K. J. Kim, J. S. Lee and C. Park, *Macromol. Chem. Phys.*, 2008, **210**, 951.

29. D. Mandal, K. J. Kim and J. S. Lee, *Langmuir*, 2012, **28**, 10310.

30. R. J. Crecorio and M. Cestari, *J. Polym. Sci. Part B: Polym. Phys.*, 1994, **32**, 859.

31. Y. Wu, Q. Gu, G. Ding, F. Tong, Z. Hu and A. M. Jonas, *ACS Macro Lett.*, 2013, **2**, 535.

32. I. D. Kim, Y. Avrahami, H. L. Tuller, Y. B. Park, M. J. Dicken and H. A. Atwater, *Appl. Phys. Lett.*, 2005, **86**, 192907.

33. H. Shin and J. T. Song, *Journal of the Korean Physical Society*, 2010, **56**, 580.

34. J. S. Sekhon, L. Aggarwal and G. Sheet, *Appl. Phys. Lett*., 2014, **104**, 162908.

35. S. Jesse, P. Baddorf and S. V. Kalinin, *Appl. Phys. Lett*., 2006, **88**, 062908.

36. P. Sharma, T. J. Reece, S. Ducharme, and A. Gruverman, *Nano Lett*. 2011, **11**, 1970.

TOC Graphic:

Ordered β-phase of PVDF is obtained by just increasing the number Langmuir-Schaefer layers, which show ferroelectric switching and piezoelectric behavior.